Stochastic resonance in vertical-cavity surface-emitting lasers based on a multiple time-scale analysis

Bob Nagler,* Michael Peeters, Irina Veretennicoff, and Jan Danckaert
Department of Applied Physics and Photonics (TW-TONA), Vrije Universiteit Brussel, Pleinlaan 2, B-1050 Brussel, Belgium
(Received 21 January 2003; published 19 May 2003)

We provide analytical evidence of stochastic resonance in polarization switching vertical-cavity surface-emitting lasers (VCSELs). We describe the VCSEL by a two-mode stochastic rate equation model and apply a multiple time-scale analysis. We were able to reduce the dynamical description to a single stochastic differential equation, which is the starting point of the analytical study of stochastic resonance. We confront our results with numerical simulations on the original rate equations, validating the use of a multiple time-scale analysis on stochastic equations as an analytical tool.

DOI: 10.1103/PhysRevE.67.056112 PACS number(s): 42.60.Mi, 42.55.Sa, 42.65.Sf, 42.50.−p

I. INTRODUCTION

As early as 1981, Benzi *et al.* [1,2] and Nicolis and Nicolis [3] introduced the concept of stochastic resonance to explain the periodicity of ice ages. Due to the modulation of the earth's eccentricity caused by the planetary gravitational pull, the flux of sunlight hitting the earth varies about 0.1% over a period of 10^5 years. The combination of this weak variation with the yearly (stochastic) change of the solar activity can trigger big climate changes. The phenomenon, that the presence of noise can increase the effect of a small modulation, is called stochastic resonance. Stochastic resonance has been extensively studied in the adiabatic limit [4–7] and in the linear response limit [4]. Furthermore, it has triggered a thorough investigation of driven time-dependent stochastic systems in the full nonadiabatic limit and beyond the linear response treatment [8,9]. It has since been experimentally observed in systems as diverse as the mechanoreceptor in the tail fan of crayfish [10] and the dispersion of particles suspended in time-periodic flows. [11]. It nowadays plays an important role in biophysical applications [12,13]. Gammaitoni *et al.* [14] gave an excellent overview of both theoretical and experimental realizations.

Recently, stochastic resonance has also been observed in vertical-cavity surface-emitting semiconductor lasers (VCSELs) [15,16]. VCSELs operating in the fundamental transverse mode usually emit light in one of two specific orthogonal linear polarizations states [17–21]. In some devices the emitted polarization changes at a specific (switching) current. Around this switching current there is a small region where spontaneous mode hopping is observed between the two modes [22–25]. When the current is modulated in this region, stochastic resonance can be observed [15,16].

In this paper we theoretically investigate stochastic resonance in VCSELs, analyzing a two-mode rate equation model that was successfully used to describe polarization switching in VCSELs [26,27]. Applying a multiple time-scale analysis (MTSA), we reduce the set of stochastic equations to a single stochastic differential equation. Although a MTSA is mostly used to simplify deterministic equations [28], it has been successfully used in the past to approximate stochastic equations [29]. Also stochastic averaging, which bears a close relation to MTSA, has been used to simplify stochastic problems [30]. We present the reduction of the set of stochastic equations in Sec. II, and we compare the theoretically derived switching times with numerical simulations of the full model in Sec. III. In Sec. IV A we show the existence of stochastic resonance using a simplified two-state model introduced by McNamara and Wiesenfeld in Ref. [4]. In an alternative approach (Sec. IV B), we analyze the residence time distribution and show stochastic resonance with the use of an indicator similar to those proposed in Refs. [7,15,31], before we conclude in Sec. V.

II. STOCHASTIC RATE EQUATIONS

We model the polarization behavior of VCSELs with the following rate equations that describe the evolution of the carrier density (N) and the photon density in the two polarization modes (P_y and P_x) [26,27]:

$$\frac{dP_x}{dt'} = [\Gamma_x a_x (N-N_t)(1-e_{sx}P_x - e_{xy}P_y) - \tau_{px}^{-1}]P_x + \beta_{sp,x}N + \tilde{F}_x', \tag{1}$$

$$\frac{dP_y}{dt'} = [\Gamma_y a_y (N-N_t)(1-e_{sy}P_y - e_{yx}P_x) - \tau_{py}^{-1}]P_y + \beta_{sp,y}N + \tilde{F}_y', \tag{2}$$

$$\frac{dN}{dt'} = \frac{I}{q_e V} - \frac{N}{\tau_c} - a_x(N-N_t)(1-e_{sx}P_x - e_{xy}P_y)P_x - a_y(N-N_t)(1-e_{sy}P_y - e_{yx}P_x)P_y + \tilde{F}_N'. \tag{3}$$

Here $e_{sy,sx,xy,yx}$, $\Gamma_{x,y}$, $a_{x,y}$, $\tau_{px,y}$, N_t, and $\beta_{sp,x,y}$ represent the gain saturation coefficients, confinement factors, the gain coefficients, the photon lifetimes, the transparency carrier

*Electronic address: Bob.Nagler@vub.ac.be;
URL: http://www.tona.vub.ac.be

density, and the noise strength for each mode. In the carrier equation, I, q_e, and V are the injected current, the elementary charge, and the volume of the active region. All the stochastic equations in this paper have to be interpreted in the Stratonovich sense [32]. The autocorrelation of the noise is given by

$$\langle \tilde{F}'_x(t')\tilde{F}'_x(s')\rangle = 4\beta_{sp,x}NP_x\delta(t'-s'), \tag{4}$$

$$\langle \tilde{F}'_y(t')\tilde{F}'_y(s')\rangle = 4\beta_{sp,y}NP_y\delta(t'-s'), \tag{5}$$

$$\langle \tilde{F}'_x(t')\tilde{F}'_y(s')\rangle = 0. \tag{6}$$

As the polarization modes in a VCSEL are nearly degenerate and have nearly equal parameters, we reduce these equations taking advantage of the different time scales of the model [26,27,33]. We reduce the time with respect to the carrier lifetime, and define a small parameter ρ,

$$t = \frac{t'}{\tau_c}, \quad \rho = \frac{\tau_{px}}{\tau_c} \simeq 10^{-3}. \tag{7}$$

As we are interested in phenomena that occur above threshold, we reduce the current to its threshold value. As the carrier density is nearly clamped above threshold, we call $\rho\eta$ the small deviation from this clamped value. This leads to

$$J = \frac{I}{I_{th}} - 1 \quad \text{with} \quad I_{th} = \frac{(1+\tau_{px}\Gamma_x a_x N_t)q_e V}{\tau_{px}\Gamma_x a_x}, \tag{8}$$

$$\eta = \rho^{-1}(\tau_{px}\Gamma_x a_x N - 1). \tag{9}$$

We, furthermore, express the photon densities in the dimensionless variables p_x and p_y,

$$p_{x,y} = \tau_c a_{x,y} P_{x,y}, \tag{10}$$

and we exploit the fact that the saturation is a small effect (e.g., $e_{sx}P_x \ll 1$), defining the following dimensionless saturation coefficients:

$$\varepsilon_{ij} = \rho^{-1}\tau_c^{-1}a_j^{-1}e_{ij}, \text{ where } i,j \in \{x,y\}. \tag{11}$$

Also, the relative gain difference between the two modes is small due to the symmetry of the device, which leads to the definition of the (current dependent) linear dichroism $G(J)$,

$$G(J) = \rho^{-1}\frac{\tau_{py}\Gamma_y a_y - \tau_{px}\Gamma_x a_x}{\tau_{px}\Gamma_x a_x}. \tag{12}$$

We suppose the current dependence is as follows:

$$G(J) = g\left(1 - \frac{J}{J_s}\right), \tag{13}$$

which implies that there is polarization switch in the neighborhood of J_s.

As the carrier density is clamped, the mean of the spontaneous emission, which is small compared to the stimulated emission, can be taken constant above threshold, leading to

$$R_{sp} = \rho^{-1}\frac{2\tau_c}{\Gamma_x}(1+\tau_{px}\Gamma_x a_x N_t)\beta_{sp}, \tag{14}$$

where we have taken $\beta_{sp} = \beta_{sp,x} = \beta_{sp,y}$.

Substituting Eqs. (7)–(14) in Eqs. (1)–(3), neglecting terms in ρ^2 and higher, we find

$$\frac{dp_x}{dt} = p_x[\eta - \varepsilon_{sx}p_x - \varepsilon_{xy}p_y] + \frac{1}{2}R_{sp} + \tilde{F}_x, \tag{15}$$

$$\frac{dp_y}{dt} = p_y[\eta + G(J) - \varepsilon_{sy}p_y - \varepsilon_{yx}p_x] + \frac{1}{2}R_{sp} + \tilde{F}_y, \tag{16}$$

$$\frac{d\eta}{dt} = \frac{J - p_x - p_y}{\rho} - \eta - p_x[\eta - \varepsilon_{sx}p_x - \varepsilon_{xy}p_y] - p_y[\eta - \varepsilon_{sy}p_y - \varepsilon_{yx}p_x] + \tilde{F}_n \tag{17}$$

with

$$\langle \tilde{F}_x(t)\tilde{F}_x(s)\rangle = 2R_{sp}p_x\delta(t-s), \tag{18}$$

$$\langle \tilde{F}_y(t)\tilde{F}_y(s)\rangle = 2R_{sp}p_y\delta(t-s), \tag{19}$$

$$\langle \tilde{F}_x(t)\tilde{F}_y(s)\rangle = 0. \tag{20}$$

We now further reduce Eqs. (15)–(17), using the same approach as in Refs. [26,33]. To leading order in ρ, Eq. (17) yields a conservation relation, stating that the total photon density equals the reduced current above threshold on the time scale of the carrier lifetime,

$$p_x + p_y = J. \tag{21}$$

The fluctuation of the photon densities in both modes are hence anticorrelated, as experimentally observed [23,24,34]. Taking the time derivative of Eq. (21) and substituting Eqs. (15) and (16) yields an expression for the carrier inversion for a constant current,

$$\eta = \frac{1}{J}[-2p_y^2\delta + (2J\delta - G)p_y + \varepsilon_{sx}J^2 - R_{sp} - \tilde{F}_x - \tilde{F}_y], \tag{22}$$

where δ is defined by

$$\delta = \varepsilon_{xy} - \varepsilon_{sx} = \varepsilon_{yx} - \varepsilon_{sy}. \tag{23}$$

We assume that $\varepsilon_{sx} = \varepsilon_{sy}$ and $\varepsilon_{xy} = \varepsilon_{yx}$, which is reasonable for VCSELs [26]. Substitution of Eqs. (22) and (21) in Eq. (16) yields a single dynamical equation:

$$\dot{p}_y = C(p_y) + \tilde{F}(p_y) \tag{24}$$

with a deterministic drift term

$$C(p_y) = p_y(J - p_y)\left(\frac{2\delta}{J}p_y - \delta + \frac{G}{J}\right) + \frac{R_{sp}}{2J}(J - 2p_y) \tag{25}$$

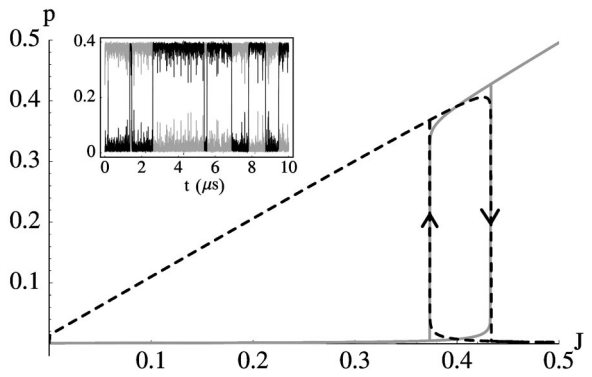

FIG. 1. Numerical solution of Eqs. (15)–(17) with a ramping current. There is a region of bistability. Parameter values, corresponding to realistic VCSEL parameters [27], are $\varepsilon_{sx}=\varepsilon_{sy}=4$, $\varepsilon_{xy}=\varepsilon_{yx}=8$, $g=14$, $J_s=0.4$, $R_{sp}=0.023$, and $\rho=10^{-3}$. The inset is a numerical time trace in the middle of the bistable region at $J=J_s$, showing the random hopping between the two polarization modes. The black (dashed) curves correspond to the p_y mode, and the gray curves to the p_x modes. The bistability is traced on the dashed p_y curve.

and a multiplicative white Gaussian noise term

$$\tilde{F}(p_y)=\tilde{F}_y-\frac{\tilde{F}_x+\tilde{F}_y}{J}p_y. \tag{26}$$

Equations (24)–(26) are the result of the MTSA approach, and describe the dynamics of the system on the time scale of our reduction (i.e., the carrier lifetime) and slower. Faster dynamics, such as the relaxation oscillations, are no longer present in our one-dimensional (1D) reduction. Note that we neglected the time evolution of the current. This approximation is valid, if we harmonically modulate the current with a pulsation significantly smaller than τ_c^{-1}. As we will never modulate above 10 MHz, we can safely make this approximation.

The stationary solutions of Eqs. (15)–(17) and their stability can be found in Refs. [26,33]. We briefly summarize the results here. When the spontaneous emission is neglected (i.e., $R_{sp}=0$), Eqs. (24) and (25) clearly show that two kinds of lasing solutions exist: two pure mode solutions ($p_x\simeq 0$, $p_y\simeq J$ and $p_x\simeq J$, $p_y\simeq 0$) and a mixed-mode solution ($p_x\simeq J/2+G/2\delta$, $p_y\simeq J/2-G/2\delta$). Linear stability analysis shows that the stability of the pure mode solutions changes around the current J_s where $G(J_s)=0$. If

$$\delta>0, \tag{27}$$

the two pure mode solutions coexist in a bistable region around J_s, and the mixed-mode solution is unstable. It was shown that both band-scattering effects [35] and spin relaxation dynamics [36,37] lead to a dichroism satisfying Eq. (27).

Figure 1 shows the stable steady state solutions. We call the mode that starts lasing at threshold the p_y mode, which implies that g is positive. When the current is set at $J=J_s$, spontaneous hopping between the two pure modes occurs (see inset of Fig. 1). A detailed study of this hopping and a comparison with experiments can be found in Refs. [27,33]. Stochastic resonance takes place when we harmonically modulate the current with a period T (remember that time is expressed in units of the carrier lifetime) inside the bistable region:

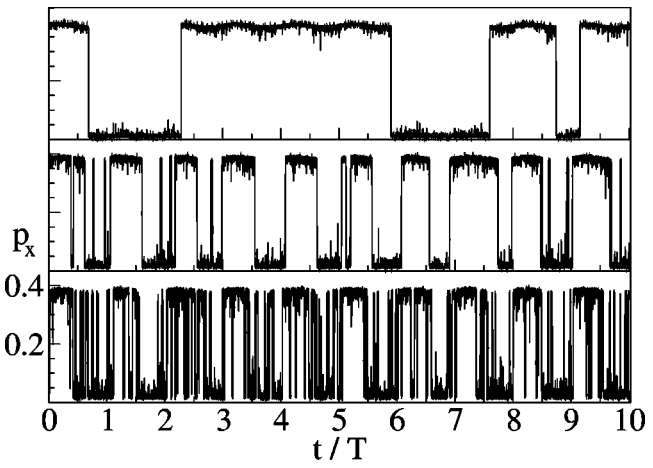

FIG. 2. Time traces of the intensity of the p_x mode for different noise strengths (from top to bottom: $R_{sp}=0.015$, 0.02, 0.03). Parameter values are $g=14$, $\varepsilon_{sx}=\varepsilon_{sy}=4$, $\varepsilon_{xy}=\varepsilon_{yx}=8$, $J=J_s+J_m\sin(\omega t)$, $J_s=0.4$, $J_m=0.005$, $\omega=10^{-6}\mathrm{s}^{-1}$ and $\rho=10^{-3}$.

$$J=J_s+J_m\sin(\omega t+\phi) \tag{28}$$

with $\omega=2\pi/T$. Time traces of one of the polarization modes can be seen in Fig. 2 for increasing noise strengths. It is clear that in the middle graph the intensity follows the modulation quite well, while in the upper graph switches are missed and in the lower graph random hopping masks the modulation. In the following section we will derive the switching rates between the two stable modes in the bistable region. These switching rates will form the basis of the theoretical approach to describe the stochastic resonance.

III. SWITCHING RATES

To obtain the switching rates between the two polarization modes, we use the Fokker-Planck equation of the probability density function of $p\equiv p_y$,

$$\frac{\partial\mathcal{P}(p,t)}{\partial t}=-\frac{\partial}{\partial p}[A(p)\mathcal{P}(p,t)]+\frac{\partial^2}{\partial p^2}[D(p)\mathcal{P}(p,t)], \tag{29}$$

where

$$\langle\tilde{F}(p,t_1)\tilde{F}(p,t_2)\rangle=2D(p)\delta(t_1-t_2) \tag{30}$$

with the diffusion coefficient $D(p)$ given by [combining the two noise terms of Eq. (26)]

$$D(p)=\frac{R_{sp}}{J}p(J-p) \tag{31}$$

and the drift coefficient $A(p)$ [using Eq. (25)]:

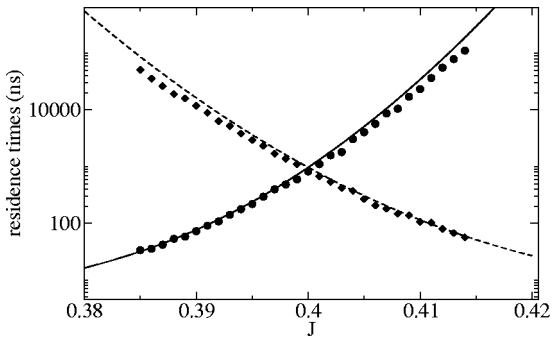

FIG. 3. The residence times of the p_x (full line and circles) and p_y (dashed line and diamonds) modes throughout the bistable region. Comparison of Eq. (39) (lines) with numerical simulation of Eqs. (15)–(17) (circles and diamonds). For the numerical points, the average is taken over 500 switches. Parameter values are $g=14$, $\varepsilon_{sx}=\varepsilon_{sy}=4$, $\varepsilon_{xy}=\varepsilon_{yx}=8$, $R_{sp}=0.023$, $J_s=0.4$, and $\rho=10^{-3}$.

$$A(p)=C(p)+\frac{1}{2}\frac{dD(p)}{dp} \tag{32}$$

$$=p_y(J-p_y)\left(\frac{2\delta}{J}p_y-\delta+\frac{G}{J}\right)+\frac{R_{sp}}{J}(J-2p_y). \tag{33}$$

The stationary solution of Fokker-Planck equation (29) is:

$$\mathcal{P}_s(p)=Qe^{-\mathrm{U}(p)} \tag{34}$$

with Q a normalization coefficient and the double-well potential $U(p)$ defined as

$$U(p)=-\int\frac{C(p)}{D(p)}dp+\frac{1}{2}\ln[D(p)] \tag{35}$$

$$=\frac{\delta}{R_{sp}}p\left(J-p-\frac{G}{\delta}\right). \tag{36}$$

We will call $p\simeq J$ mode the "+" state and $p\simeq 0$ the "−" state. Using the potential solution, the mean residence times of the two modes can be derived [38]. As $\mathcal{P}_s^{-1}(p)$ is sharply peaked around the maximum of the potential, we can get the following approximate expressions for the residence times [39]:

$$t_-=2D(p_{\max})^{-1}\int_0^{p_{\max}}\mathcal{P}_s(p)dp\int_0^{p_{\max}}\mathcal{P}_s(p)^{-1}dp, \tag{37}$$

$$t_+=2D(p_{\max})^{-1}\int_{p_{\max}}^{J}\mathcal{P}_s(p)dp\int_{p_{\max}}^{J}\mathcal{P}_s(p)^{-1}dp. \tag{38}$$

Using Eqs. (34) and (35), we get [43]

$$t_\pm=\frac{2J\pi\delta}{J^2\delta^2-G^2}\mathrm{erf}\left(\frac{G\pm J\delta}{2\sqrt{R_{sp}\delta}}\right)\mathrm{erfi}\left(\frac{G\pm J\delta}{2\sqrt{R_{sp}\delta}}\right). \tag{39}$$

In Fig. 3 we compare Eq. (39) with numerical simulations of Eqs. (15)–(17). We see that the residence times scale over three orders of magnitude with the current. In the whole region the correspondence between the numerical and the analytical approach is quite good. However, for large residence times, the analytical predictions are consistently higher than the numerical simulations. The discrepancy always remains smaller than 10%.

This discrepancy is not present when comparing the theory with the 1D simulations on the basis of Eq. (24), which match exactly (not shown). Numerical simulations have also ruled out the condensation of the noise terms into one in Eq. (26) as a source of error. Also, modified integrations of the system with colored noise show that it is not the use of white noise in the MTSA which is flawed. We suspect that the use of the conservation relation, Eq. (21), in the autocorrelation of the combined noise term in Eq. (26) is causing some unintentional correlation. This hypothesis is consistent with the fact that inserting a minor amount (5%) of correlation between the two noise sources (i.e., $\tilde{F}_x$ and $\tilde{F}_y$) in the 3D equations increases the residence times. The needed amount of correlation to match the theory and the numerics seems to be a function of the reduced current. A more detailed analysis of the consequences of applying a MTSA on stochastic equations remains an open issue, but lies outside the scope of this paper. For the purpose of this work, the obtained agreement between the numerical simulation of the 3D model and the analytical result based on the reduction is more than sufficient.

IV. ANALYSIS OF THE STOCHASTIC RESONANCE

In this section we will show the presence of stochastic resonance in two ways: we will first use a simplified two-state model introduced by Ref. [4], and alternatively use an indicator based on the distribution of the residence times of the two modes. Both methods take the mean residence time [Eq. (39)] as a starting point.

A. Two-state model

As the intra-well relaxation time of p is much shorter than the residence times, we can make a two-state approximation: we model the continuous system as being in either the off state, or the on state, filtering all the information except in which potential well the particle resides at time t [4]. This approach only holds in the adiabatic limit when the frequencies are small [9] (this is no problem in the context of this paper since the MTSA is also only valid for small frequencies and we never modulate the current with frequencies larger than 10 MHz). We define $n_+(t)$ and $n_-(t)$ as the probability that the system is in the p_y or p_x state at time t. We have, of course, the normalization condition

$$n_+(t)+n_-(t)=1. \tag{40}$$

These probabilities change according to the following two master equations [4,14]:

$$\dot{n}_\pm(t)=W_\pm(t)n_\mp(t)-W_\mp(t)n_\pm(t). \tag{41}$$

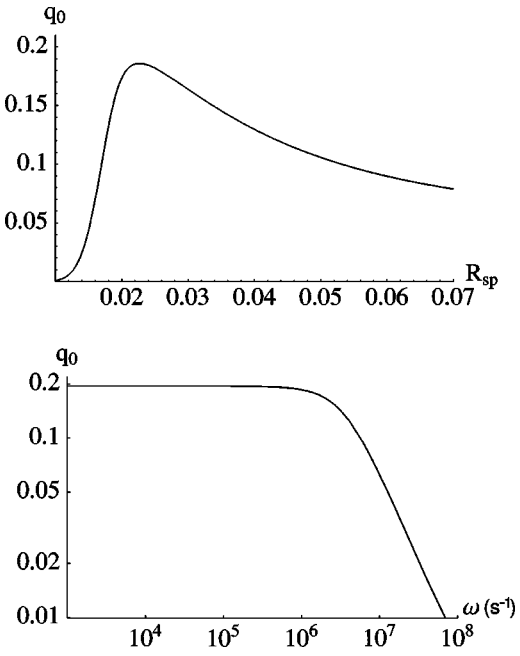

FIG. 4. Parameter q_0 as a function of R_{sp} (top) and ω (bottom). Parameter values are $\delta=4$, $g=14$, $J=J_s+J_m\sin(\omega t)$, $J_s=0.4$, $J_m=0.005$, $\omega=10^6$ s^{-1} in the top graph, and $R_{sp}=0.023$ in the bottom graph. Perfect synchronization would give a value of $q_0=2J_s/\pi$.

In Eq. (41), $W_{\pm}(t)$ are the switching rates to the on/off state, i.e., the inverse of the residence times in Eq. (39),

$$W_{\pm}(t)=t_{\mp}(t)^{-1}. \tag{42}$$

If we modulate the current, these rates will indeed depend sinusoidally on the time. Solving Eq. (41) gives [4]

$$n_{\pm}(t)=g(t)\left[n_{\pm}(t_0)+\int_{t_0}^{t}W_{\pm}(\tau)g^{-1}(\tau)d\tau\right], \tag{43}$$

$$g(t)=\exp\left(-\int_{t_0}^{t}[W_{\pm}(\tau)+W_{\mp}(\tau)]d\tau\right). \tag{44}$$

For large t, $n_{\pm}$ will become periodic with the same frequency as the current modulation [44].

The average of the intensity of one of the polarization modes is approximately (assuming that $p=0$ in the off state and $p=J$ in the on state)

$$\langle p\rangle=p_{\mathrm{off}}n_{-}+p_{\mathrm{on}}n_{+}\simeq J_s n_{+}. \tag{45}$$

We define q_0 as the first Fourier coefficient of Eq. (45). The quantity q_0 is essentially identical to the ''spectral amplification'' introduced in [8,9] Fig. 4, q_0 is plotted as a function of the noise strength for a constant frequency, and as a function of the frequency for a constant noise strength, showing the typical stochastic resonance. The generic model with a quartic potential of McNamara and Wiesenfeld [4] predicts that stochastic resonance occurs at a period of oscillation twice the value of the residence time $t_{\pm}$ in the middle of the modulation region. This is only true for exceedingly small modulation amplitudes. Indeed, for the parameters of Fig. 4, the generic model would lead to stochastic resonance for a noise strength of $R_{sp}=0.0194$, whereas Fig. 4 shows that the actual value is about $R_{sp}=0.023$. An in depth treatment of the influence of the magnitude of the modulation amplitude on the stochastic resonance peak can be found in Refs. [9,40].

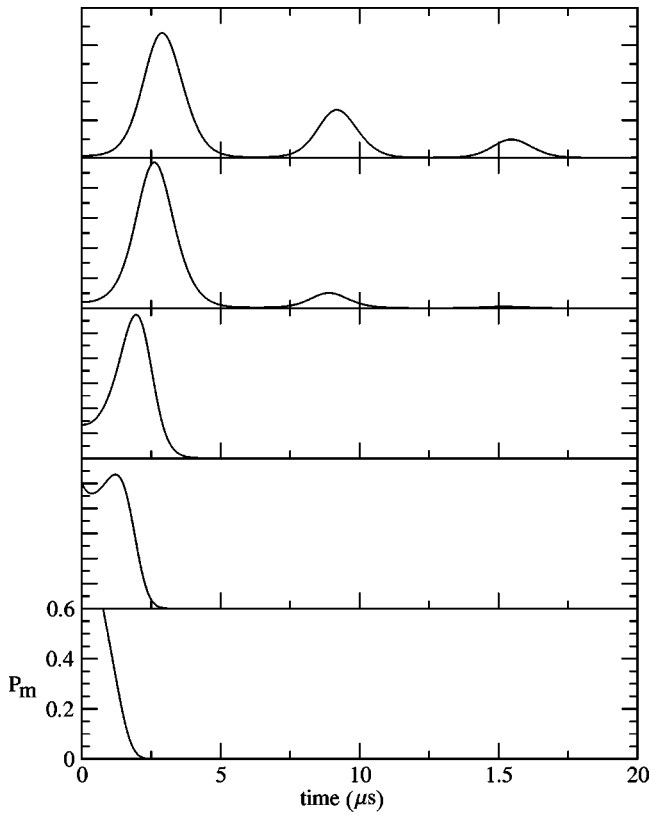

FIG. 5. Distribution of the residence time for a modulation pulsation of 10^6 s^{-1} for various noise strengths (from top to bottom $R_{sp}=0.16$, 0.18, 0.22, 0.26, 0.30). Other parameter values are $\delta=4$, $g=14$, $J=J_s+J_m\sin(\omega t)$, $J_s=0.4$, and $J_m=0.005$.

B. Residence time distribution

Another way to investigate stochastic resonance is to look at the statistical properties of the residence times [6,31,41,42]. When the potentials are constant, the residence times have the usual exponential distribution. If the current is modulated sinusoidally as in Eq. (28), this distribution has the form [45]

$$P_{m_{\pm}}(t)=t_{\pm}(J)^{-1}\exp\left(-\int_0^t\frac{ds}{t_{\pm}(J)}\right). \tag{46}$$

$P_{m_{\pm}}$ can be seen in Fig. 5 for increasing noise strengths. The first peak in the distribution functions represent switches that are synchronized with the modulation signal, whereas the following peaks represent events where the system did not switch for one or more periods. For high noise strengths the peaks disappear and the exponential distribution of the unmodulated system appears. It should be noted that this dis-

tribution is not really the distribution of the residence times. It is the distribution of the time you stay in the p_y mode if you are in that mode at time $t=0$. So it is only the residence time of the p_y mode, when the laser switched to that mode at time $t=0$, or in other words, when the phase of the sine modulation equaled ϕ. To get the distribution of the phase independent residence time, $P_{r_\pm}(t)$, we have to average over all possible phases (we write the dependence of $P_{m_\pm}$ on ϕ explicitly),

$$P_{r_\pm}(t)=\int P_{m_\pm}(t,\phi)P_\phi(\phi)d\phi, \tag{47}$$

where $P_\phi(\phi)$ is the probability density that you switched to the p_y mode at phase ϕ of the current modulation. Unfortunately, there is no known method to derive this phase distribution P_ϕ, although in some limits self-consistent distributions have been proposed in the literature [5–7,14].

We now introduce an indicator to show the presence of stochastic resonance, which is based on the indicators defined in Refs. [7,15,42]. We calculate the area under the peaks at $T/2$, $3T/2$, etc., after subtraction of the background:

$$I_n=\int_{nT-3/4T}^{nT-1/4T}\{P_m(J=J_0+J_m\sin[\omega t])-P_m(J=J_0)\}dt. \tag{48}$$

In contrast to the indicators in Refs. [7,15,42], we use the phase dependent distribution $P_{m_\pm}$ and take $\phi=0$, as we have no analytical expression of the phase independent distribution $P_{r_\pm}$. Furthermore, $\phi=0$ corresponds to the zero crossing of the current modulation, which is easy to take as a trigger level in experiments. We have a stochastic resonance if the indicator I_1 attains a maximum, while the others (i.e., I_2, I_3, ...) do not.

In Fig. 6 we plot I_1, I_2 and I_3 as a function of the frequency (for constant noise strength) and as a function of the noise strength (for constant frequency). We see that stochastic resonance appears both as a function of the noise strength and as a function of the frequency (also called bona fide resonance [42]).

Note that, similar to Refs. [15,16], there is a small difference between the optimal value for resonant behavior of q_0 (see Sec. IV A) and the optimal value for resonant behavior of the indicator I_1.

V. CONCLUSION

In this paper we have theoretically studied stochastic resonance in VCSELs. Our study was based on an intensity rate equation model that has been used in the past to successfully model the polarization characteristics in VCSELs.

To get the theoretical results we used a MTSA on the stochastic rate equation model. Although there is no rigorous mathematical justification for applying a MTSA on stochastic differential equations, it provides valid results. We were able to reduce the three rate equations to a single stochastic differential equation, from which analytical expressions for the potential and the switching times were derived. We have checked the analytical results with numerical simulations.

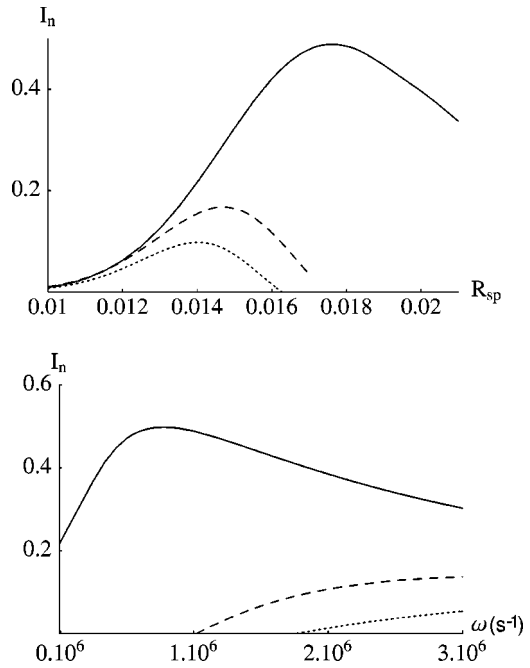

FIG. 6. Indicators I_n [see Eq. (48)] of stochastic resonance, based on the integral over half a period of the probability density function after subtraction of the background noise. The top figure shows the indicator as a function of R_{sp} for a constant pulsation ($\omega=10^6$ s^{-1}), the bottom figure shows the indicator as a function of the pulsation for a constant noise strength ($R_{sp}=0.0175$). The black, dashed, and dotted curves correspond to I_1, I_2, and I_3. We see stochastic resonance of I_1 around $R_{sp}=0.0175$ in the top figure, and around $\omega=0.9\ 10^6$ s^{-1} in the bottom figure. Parameter values are $\delta=4$, $g=14$, $J=J_s+J_m\sin(\omega t)$, $J_s=0.4$, and $J_m=0.005$.

Stochastic resonance occurs between two stable polarization states. We have analyzed the resonance in two ways. We first used a two-state model that only considers in which potential minimum (corresponding to either the p_x or the p_y polarization state) the system is. Alternatively, we have proposed an indicator, similar to the ones previously proposed in Refs. [5–7,14], based on the residence time distribution. The indicator shows a resonant behavior both as a function of the noise strength and as a function of the frequency, the so called bona fide resonance.

ACKNOWLEDGMENTS

This research was supported by the Belgian Office for Scientific, Technical and Cultural Affairs in the framework of the Inter-university Attraction Pole Program, the Fund for Scientific Research—Flanders (FWO-V), the Concerted Research Action ''Photonics in Computing,'' the research council (OZR) of the VUB, and EU RTN network VISTA (contract No. HPRN-CT-2000-00034). We would like to thank Francesco Marin for many helpful discussions.

[1] R. Benzi, A. Sutera, and A. Vulpiani, J. Phys. A **14**, 453 (1981).
[2] R. Benzi, G. Parisi, A. Sutera, and A. Vulpiani, Tellus **34**, 10 (1982).
[3] C. Nicolis and G. Nicolis, Tellus **33**, 225 (1981).
[4] B. McNamara and K. Wiesenfeld, Phys. Rev. A **39**, 4854 (1989).
[5] R. Löfstedt and S.N. Coppersmith, Phys. Rev. Lett. **72**, 1947 (1994).
[6] R. Löfstedt and S.N. Coppersmith, Phys. Rev. E **49**, 4821 (1994).
[7] M.H. Choi, R.F. Fox, and P. Jung, Phys. Rev. E **57**, 6335 (1998).
[8] P. Jung and P. Hänggi, Europhys. Lett. **8**, 505 (1989).
[9] P. Jung and P. Hänggi, Phys. Rev. A **44**, 8032 (1991).
[10] J.K. Douglass, L. Wilkens, E. Pantazelou, and F. Moss, Nature (London) **365**, 337 (1993).
[11] I. Claes and C. van den Broeck, Phys. Rev. A **44**, 4970 (1991).
[12] K. Wiesenfeld and F. Jaramillo, Chaos **8**, 539 (1998).
[13] P. Hänggi, ChemPhysChem **3**, 285 (2002).
[14] L. Gammaitoni, P. Hänggi, P. Jung, and F. Marchesoni, Rev. Mod. Phys. **70**, 223 (1998).
[15] G. Giacomelli, F. Marin, and I. Rabbiosi, Phys. Rev. Lett. **82**, 675 (1999).
[16] S. Barbay, G. Giacomelli, and F. Marin, Phys. Rev. E **61**, 157 (2000).
[17] K.D. Choquette, D.A. Richie, and R.E. Leibenguth, Appl. Phys. Lett. **64**, 1062 (1994).
[18] J. Martin-Regalado, F. Prati, M. San Miguel, and N.B. Abraham, IEEE J. Quantum Electron. **33**, 765 (1997).
[19] K. Panajotov, B. Ryvkin, J. Danckaert, M. Peeters, H. Thienpont, and I. Vertennicoff, IEEE Photonics Technol. Lett. **10**, 6 (1998).
[20] M.P. van Exter, A. Al-Remawi, and J.P. Woerdman, Phys. Rev. Lett. **80**, 4875 (1998).
[21] T. Ackemann and M. Sondermann, Appl. Phys. Lett. **78**, 3574 (2001).
[22] M.B. Willemsen, M.U.F. Khalid, M.P. van Exter, and J.P. Woerdman, Phys. Rev. Lett. **82**, 4815 (1999).
[23] G. Giacomelli and F. Marin, Quantum Semiclassic. Opt. **10**, 469 (1998).
[24] G. Giacomelli, F. Marin, M. Gabrysch, K.H. Gulden, and M. Moser, Opt. Commun. **146**, 136 (1998).
[25] G. Verschaffelt *et al.*, Proc. SPIE **3946**, 246 (2000).
[26] J. Danckaert, B. Nagler, J. Albert, K. Panajotov, I. Veretennicoff, and T. Erneux, Opt. Commun. **201**, 129 (2002).
[27] B. Nagler, M. Peeters, J. Albert, G. Verschaffelt, K. Panajotov, I. Veretennicoff, and J. Danckaert Phys. Rev. A (to be published).
[28] S.H. Strogatz, *Nonlinear Dynamics and Chaos* (Perseus Books, Cambridge, MA, 1994).
[29] P. Jung and P. Hänggi, Phys. Rev. A **35**, 4464 (1987).
[30] P. Hänggi and P. Riseborough, Am. J. Phys. **51**, 347 (1983).
[31] L. Gammaitoni, F. Marchesoni, E. Menichella-Saetta, and S. Santucci, Phys. Rev. Lett. **62**, 349 (1989).
[32] H. Risken, *The Fokker-Planck Equation* (Springer-Verlag, Berlin, 1996).
[33] B. Nagler, J. Danckaert, J. Albert, M. Peeters, K. Panajotov, I. Veretennicoff, and T. Erneux, Proc. SPIE **4283**, 275 (2001).
[34] M.P. van Exter, M.B. Willemsen, and J.P. Woerdman, Phys. Rev. A **58**, 4191 (1998).
[35] B.M. Yu and J.M. Liu, J. Appl. Phys. **69**, 7444 (1991).
[36] M.P. van Exter, M.B. Willemsen, and J.P. Woerdman, J. Opt. B: Quantum Semiclassical Opt. **1**, 637 (1999).
[37] G. Van der Sande, J. Danckaert, I. Veretennicoff, and T. Erneux, Phys. Rev. A **67**, 013809 (2003).
[38] P. Hänggi, P. Talkner, and M. Borkovec, Rev. Mod. Phys. **62**, 251 (1990); **62**, 174 (1990); **62**, 290 (1990).
[39] C.W. Gardiner, *Handbook of Stochastic Methods for Physics and Natural Sciences* (Springer-Verlag, Berlin, 1983), pp. 139 and 140.
[40] R.F. Fox and Y. Lu, Phys. Rev. E **48**, 3390 (1993).
[41] T. Zhou and F. Moss, Phys. Rev. A **41**, 4255 (1990).
[42] L. Gammaitoni, F. Marchesoni, and S. Santucci, Phys. Rev. Lett. **74**, 1052 (1995).
[43] The error function and the imaginary error function are defined by $\mathrm{erf}(x)=2/\sqrt{\pi}\int_0^x e^{-t^2}dt$ and $\mathrm{erfi}(x)=-i\,\mathrm{erf}(ix)$.
[44] It can be shown [4,14] that for a small modulation in a quartic potential, the mean of the stochastic variable is for large times approximately $\langle x\rangle=\overline{x}\cos(\Omega t+\overline{\phi})$ with $\overline{x}=Ax_m^2/D2r_k/\sqrt{2r_k^2+\Omega^2}$, where $\pm x_m$ are the minima of the potential, r_k is the escape rate without modulation, Ω is the modulation frequency, and D is the noise diffusion coefficient.
[45] This is the case if $\int_0^\infty t_\pm(t)^{-1}dt=\infty$, which is always true in this paper.